

Pseudopotential Periodic Hartree–Fock Study of K_8In_{11} and Rb_8In_{11} Systems

R. Llusar,* A. Beltrán, and J. Andrés

Department of Experimental Sciences, University Jaume I, Box 242, 12080 Castelló, Spain

B. Silvi and A. Savin

Laboratoire de Dynamique des Interactions Moléculaires (UPR271), Université Pierre et Marie Curie, 4, Place Jussieu, 75252 Paris Cédex, France

Received: March 23, 1995; In Final Form: June 8, 1995*

The bonding in K_8In_{11} and Rb_8In_{11} has been investigated at the SCF level with the periodic Hartree–Fock method. Comparison is made with In_{11} clusters with formal charges 7– and 8– calculated at the same level. The structure of the 7– cluster has been optimized; it significantly differs from the structure observed in the condensed phase. The second anion (8–) is found to be dissociative. Moreover, the indium Mulliken populations in clusters are dramatically different from those calculated for the solid phase. This indicates that the reliability of the cluster approach is highly questionable. The stability of the solid phases is mostly due to the electrostatic interactions between the anionic clusters and the alkali counterions. The integrated charge density in the cation region is consistent with a picture in which an electron is delocalized over the potassium layers. The band structure and density of states of the solid phases are discussed. Both K_8In_{11} and Rb_8In_{11} are found to be weak electronic conductors. At the present state of the art, it is not possible to assess the charge borne by the indium cluster and, therefore, to decide whether one or more electrons are delocalized over potassium layers. The bonding in these systems has been investigated from the topological analysis of the electron localization function point of view. The bonding in the In_{11} anionic clusters is characterized by a network of attractors lying 1 Å outward from the indium centers.

Introduction

The clustering of main group metals in intermetallic Zintl phases is a well-documented fact in solid state chemistry which has also been more recently observed in liquid alloys.^{1,2} In addition, post-transition elements present a very rich cluster chemistry in the gas phase which greatly exceeds the number of clusters isolated in solid phases probably because of the particular thermodynamic conditions encountered in beam experiments.³

Deltahedral main group clusters are described as electron deficient, because their number of electrons is not large enough to allow the formation of localized bonds along the edges of the polyhedron. Stable clusters of the main group elements fall into two categories. On the one hand are the highly electron deficient clusters of Li and Be and, on the other hand, those formed by post-transition elements. For these latter, the classical Wade's rules which require $2n + 2$, $2n + 4$, and $2n + 6$ skeletal electrons for respectively closo, nido, and arachno M_n species are fulfilled in most cases.⁴

Isolated clusters of group 13 metallic elements would carry, especially for large n values, excessive negative charges in order to satisfy the minimum $2n + 2$ Wade's rule requirement for the M_n^{n-2} closo species. Nature provides several ways to avoid such huge negative charges, the most widespread being the formation of networks of clusters via normal intercluster bonds. Electron counting rules, taking into account the fusion and linkage of deltahedral boron and gallium clusters, have been developed on the grounds of molecular orbital and tight binding ideas.⁵ It is worth noting that the previously mentioned negative charge is more related to chemical partition of space rather than to a system of effective point charges generating an electrostatic potential.

Other alternatives have also been found for the indium and thallium intermetallic phases in which cluster distortions or bonding with a heteroatom encompassed within the cage provide solid state compounds with discrete cluster units. An interesting analogy between fullerenes and transition metal (Ni, Pd, or Pt) centered indium clusters in the indium–sodium system has been recently pointed out by Sevov and Corbett.⁶ Among these intermetallic phases, a remarkable example in which distortion leads to an unusual hypoelectronic cluster is provided by the rhombohedral A_8In_{11} ($A = K, Rb$) system.^{7,8} Isostructural analogs have been evidenced with thallium.⁸ Single crystal structure determinations reveal an unprecedented type of In_{11} polyhedra, the compressed pentacapped trigonal prisms. In this structure, layers of indium polyhedra, lying on a 3-fold axis are rhombohedrally stacked along the c axis with potassium layers both within and between the cluster layers. The application of the Zintl–Klemm concept to A_8In_{11} would result in the formulation of an In_{11}^{8-} cluster with an odd number of electrons.⁹ Conductivity and diamagnetic susceptibility⁷ measurements on the K_8In_{11} species show a metallic behavior together with a small Pauli paramagnetism consistent with the picture in which one electron per cluster unit is delocalized.⁷ The corresponding formal representation of the solid phase should then be $(K^+)_8In_{11}^{7-}(e^-)$.

From a theoretical point of view, these two compounds, namely K_8In_{11} and Rb_8In_{11} , have been studied at a semiempirical level using the extended Hückel method either on the In_{11} naked cluster⁷ or on the crystalline phases.⁸ In the cluster, the calculation places the last electron ca. 1 eV above the plausible HOMO, and to overcome this improbable result it was concluded that there were 10 bonding electron pairs and suggested that the remaining electron was delocalized over the potassium double layers. The periodic calculation of Blase *et al.*⁸ supports this interpretation. In particular, the density of

* Abstract published in *Advance ACS Abstracts*, July 15, 1995.

TABLE 1: Indium Atomic Basis Set

exponent (bohr ⁻²)	s coefficient	p coefficient
1.434 261	1.308 440	0.170 079
1.278 590	-1.611 305	-0.198 738
0.152 664	0.792 518	0.492 907
0.050 623	1.0	1.0

states matches the MO diagram of the cluster. The Fermi level corresponds to the occupation of 10 doubly occupied In–In bonding orbitals. The crystal orbital overlap population (COOP) is typical of intermetallic phases. The HOMO area is anti-bonding for In–In interactions with strong K–In interactions whereas the K–K interactions remain without chemical significance. This periodic calculation does not support that one electron should be delocalized over the K layers; instead, the excess of electron density should be assigned to K–In bonding levels in the HOMO area. However, this conclusion could be a consequence of a particular choice of the K parameters.

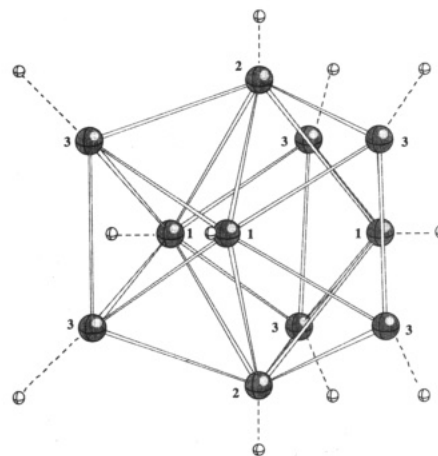
In the present paper we present preliminary results obtained at the *ab initio* level on the In₁₁ clusters and on the R $\bar{3}c$ structures. The total number of electrons (i.e., 1382 for the K₈–In₁₁ unit cell) forbid any all-electron calculation of these compounds. The inner shells of indium and potassium are not expected to play a significant role in the bonding. Therefore, the calculations have been carried out with effective core pseudopotentials allowing a significant lowering of the number of electrons explicitly taken into account. Moreover, such pseudopotentials take into account relativistic effects which can be significant for heavy elements.

In the second section, the technical details of the calculations are described. In the third section, we report and discuss the results with a particular emphasis on the comparison between periodic and isolated cluster results. Finally, in the last section we present some innovative ideas on the bonding in such materials based on the analysis of the electron localization function.¹⁰

Method of Calculation

The calculations on the two clusters In₁₁⁷⁻ and In₁₁⁸⁻ have been performed with the *ab initio* Gaussian92 software.¹¹ The very large number of electrons in these clusters, respectively 546 and 547, prevents performing all-electron calculations. Therefore, the core electrons were treated within the effective core pseudopotential framework. The pseudopotentials used in this calculations are the semilocal ones of Durand and Barthelat,¹² which include relativistic effects. A split-valence basis has been optimized, with a contraction scheme analogous to the PS-31G sets previously published for main group elements of the three first rows.¹³ The exponents and contraction coefficients are given in Table 1. The total energy calculated with this basis set for the atom is -1.811 777 5 hartrees, which is 0.12 hartree larger than the sum of the first three ionization potentials of this element. The discrepancy is partly due to the missing correlation energy which can be estimated of the order of 0.05 hartree from a calculation carried out at the DFT level with the Becke's exchange¹⁴ and Lee, Yang, and Parr correlation¹⁵ functionals.

The calculations of the solid state phases have been performed at the periodic Hartree–Fock level with the CRYSTAL92¹⁶ program developed in Torino. A documented description of the method has been published by Pisani *et al.*¹⁸ This method works within a single determinant approximation of the wave function in which the crystalline orbitals are expressed as linear combinations of Bloch functions which are themselves expressed in terms of the localized atomic basis functions of each unit

Figure 1. Geometry and localization attractors in In₁₁ clusters.

cell. As input, the program requires geometry and basis set information together with a set of thresholds which control the truncation of infinite sums and a set of shrinking factors which determines the sampling **k** points over the Brillouin zone. As output, it provides the unit cell energy, the wave function, and related one-electron properties. The program works at the all-electron (AE) level as well as with effective core pseudopotentials (ECP).

In solid phase calculations the exponents of the diffuse shell have to be reoptimized and increased in order to avoid basis set linear dependence; the value $\alpha_{opt} = 0.07$ has been used for both systems. Potassium and rubidium pseudopotentials are respectively those of Durand and Barthelat¹² and of Jeung *et al.*¹⁷ For these atoms the basis set is made by a single sp-shell, the exponent of which is 0.15. The reciprocal space integration is performed using a commensurate net, the meshes of which are determined by the shrinking factor *S*. *S* = 6, corresponding to 32 **k** points, has been used for the present calculations; when *S* = 12 is used, the energy change is less than the SCF convergence threshold 10⁻⁶.

Results and Discussion

In₁₁⁷⁻ and In₁₁⁸⁻ Clusters. In order to check the reliability of the cluster approach, a series of comparative calculations have been carried out. Starting from the solid phase structure of the In₁₁ deltahedron observed in solid phase^{7,19} which has an almost *D*_{3h} symmetry, the structure of the cluster has been optimized with this latter symmetry constraint.

The labeling of atoms follows the nomenclature of Corbett and Sevov⁷ and is displayed by Figure 1. It is well-known that SCF calculations on the polyanion do not lead to a stable state: occupied molecular orbitals have positive eigenvalues, so the addition of very diffuse basis functions would allow the supplementary electrons to be not bounded. In the solid state, the polyanion is stabilized by the crystal field. However, with a limited basis set it is possible to get some information on the bonding from the naked polyanion calculations, although the results concerning energy related properties remain questionable. Table 2 compares the independent internuclear distances in the optimized In₁₁⁷⁻ cluster structure and the equivalent experimental distances found for the crystalline phase. The bond lengths are significantly longer for the optimized isolated In₁₁⁷⁻ cluster unit.

The calculated total energy of this species is -18.309 619 8 hartrees for the optimized In₁₁⁷⁻ structure instead of -18.002 51 hartrees for the Zintl-phase unrelaxed one. Note that, without symmetry constraint, the geometry optimization yields almost

TABLE 2: Independent Interatomic Distances (Å) in In_{11} Deltahedra

	K_8In_{11} (exp ^{7,19})	optimized In_{11}^{7-} cluster ^a
In(1)–In(2)	3.284	4.082
In(1)–In(3)	3.060	3.636
In(1)–In(3)	2.967	3.636
In(2)–In(3)	3.054	3.395
In(3)–In(3)	3.102	4.235

^a The optimized cluster has a D_{3h} symmetry constraint.

the same results except for very small distortions which lower the symmetry to D_{2h} .

The In_{11}^{8-} anion has an odd number of electrons; its ground state can be a doublet or a state of higher multiplicity. In a first step, different multiplicities have been investigated for the zintl-phase geometry. The ground state is found to be a doublet, the energy of which is calculated 0.065 hartree lower than the quadruplet, with the sextuplet and octuplet being above. Attempts to find the equilibrium of the In_{11}^{8-} anion failed; the cluster tends to dissociate probably because of the excessive negative charge. Nonetheless, for the unrelaxed geometry, the energy difference between In_{11}^{8-} and In_{11}^{7-} clusters, namely the vertical electron affinity of In_{11}^{7-} , is calculated to be –0.683 hartree, i.e., –18.5 eV.

It is not possible to perform a direct comparison between the Hartree-Fock molecular orbital eigenvalues and the EHT MO diagram reported by Corbett and Sevov,⁷ because the orbital energies have different meanings in these two approaches. In particular, the order of the symmetry orbitals is quite different. Moreover, the gap between the HOMO and LUMO is 3 times larger for the SCF calculation of In_{11}^{7-} than for the EHT one. Note that the overestimation of the HOMO–LUMO gap is usual in the Hartree-Fock calculation. A DFT calculation, in which the gap is expected to be underestimated, carried out at the same geometry and with the same basis set reduces the gap to 1.02 eV, while providing the same ordering of symmetry orbital which is in the HF approximation.

Periodic Hartree-Fock Results. The periodic Hartree-Fock calculations on K_8In_{11} and Rb_8In_{11} have been performed for the experimental structures of these compounds.^{7,19} The unit cell contains two A_8In_{11} asymmetric units and, therefore, 82 valence electrons. It is not possible to perform the optimization of the structure of these systems at the present state of the art because of the size of the basis set and of the number of independent structural parameters. The unit cell energies are calculated to be –43.1527 and –43.3404 hartrees, which correspond to binding energies of –0.940 26 and –1.247 42 hartrees/cell for K_8In_{11} and Rb_8In_{11} , respectively. The cohesive energy of the lattice has mostly an electrostatic origin. A crude electrostatic model, in which a 7– or 8– negative charge is located in position 6b, and complementary positive charges which ensure the electroneutrality at the potassium positions yield electrostatic energies of –7.55 and –9.861 hartrees/cell, respectively. Adding these to the algebraic sum of the ionization potential of the potassium atoms and to the total energies of the two In_{11}^{8-} or In_{11}^{7-} clusters provides total energies falling within 1 hartree/cell.

Wave Function Analysis

The bonding in crystals (or in molecules) can be investigated by different techniques. The band structure characterizes the nature of the bonding: in closed-shell interacting structures (ionic, van der Waals, hydrogen bonded, and molecular crystals) its topology is rather flat compared to metallic and covalent

systems. The projected density of states (PDOS) and the Mulliken population analysis are based on the same projection and partition schemes and yield basically the same information: Mulliken orbital population can be recovered by integrating the PDOS. These procedures are not strongly built because they depend upon how basis functions are assigned to each atom and upon an arbitrary partition. Therefore, these kinds of analysis have to be handled with care. If the basis set is well balanced, qualitative answers allowing the assignment of the band structure and the determination of bond polarities can be obtained in this way. Though the Mulliken charges have no physical significance, their values in a series of polymorphs, calculated within the same accuracy and with identical basis sets, can be used to discuss trends.

The charge density, $\rho(r)$, is a well-defined physical quantity which has a definite value at each point of the three-dimensional direct space. In principle, it can be exactly evaluated. However, the total charge density is not very informative by itself because it is mostly dominated by the core contributions. An attractive analysis is provided by Bader's theory of atoms in molecules,²¹ which allows a sound partition of the charge density. In this theory, atomic basins are defined as parts of the space containing an electron attractor (nucleus) and limited by surfaces of zero flux in the gradient vectors of the charge density. Moreover, the topology of the charge density allows one to define bond paths and critical points. The intersection of a zero flux surface and a bond path corresponds to a bond critical point. The value of the Laplacian of the charge density at bond critical points allows to discriminate between closed-shell and electron-shared (covalent) interactions.

Recently, Becke and Edgecombe²² have proposed an electron localization function (ELF) which appears to be very attractive to discuss the bonding. The ELF is defined as

$$ELF = \frac{1}{1 + (D_o/D_o^0)^2}$$

in which D_o and D_o^0 represent the curvature of the electron pair density for electron of identical spins (the Fermi hole) for respectively the actual system and a homogeneous electron gas with the same density. Savin *et al.*²³ have proposed another interpretation. They remarked that D_o can be identified as the Pauli kinetic energy density of the actual fermionic system with respect to a bosonic system having the same density. ELF is therefore a measure of the bosonic behavior of the electron density. Where electrons are alone or form pairs of opposite spins, the Pauli principle has little influence, and they almost behave like bosons. In such regions the excess local kinetic energy is small and ELF is close to 1. At the border between these regions, the probability of finding parallel spin electrons close together is increased, and therefore ELF has a low value. The ELF displays the shell structure of atoms as well as allows to discriminate between covalent and closed-shell interactions. The topological analysis of the ELF function gradient field has given rise to a new classification of chemical bonds based on topology.^{10,24} In this theory, the ELF gradient field attractors, called hereafter localization attractors, are classified into core, valence bonding, and nonbonding attractors. A bonding attractor is a valence attractor which lies between two (or more) core attractors. This allows one, then, to define shared and unshared electron interactions according to the presence of bonding attractors.¹⁰ Moreover, the ELF gradient field enjoys structural stability:²⁰ i.e., the quality of the wave function is not very important provided it corresponds to the correct electronic state of the system. In principle, the topological analysis of the

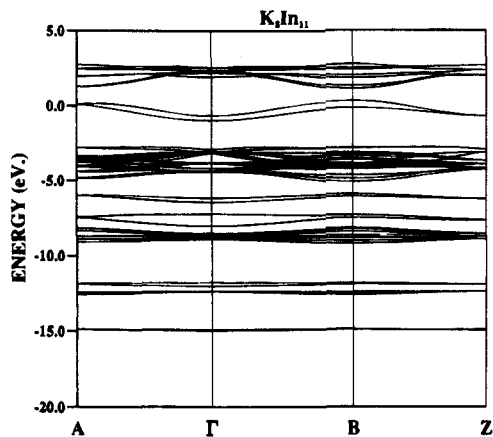


Figure 2. Band structure of K_8In_{11} . The origin of the energy scale is taken at the Fermi level.

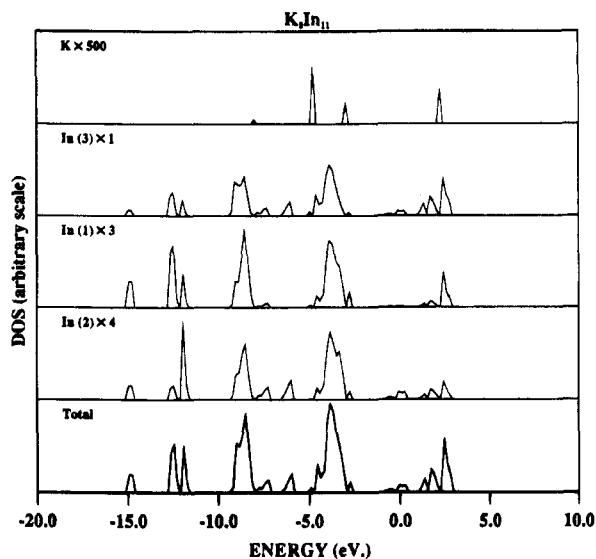


Figure 3. Projected density of states of K_8In_{11} .

density and of the ELF function is defined for all electron densities only. However, in the case of ELF, reliable qualitative answers can often be obtained from pseudopotential calculations. In this case, ELF is close to zero in the core regions, and neither the location nor the significance (bonding or nonbonding) of the valence attractors is significantly changed.

Figure 2 displays the band structure of K_8In_{11} along the high-symmetry lines of the Brillouin zone. The overall topology of this band structure is very flat and therefore characteristic of an ionic compound. The top part of the valence band, between -5 and -3 eV, corresponds to indium nonbonding $5p$ states, as can be seen from the projected density of states in Figure 3. The band at the Fermi level corresponds to the crystal orbitals delocalized over neighbor clusters and which are responsible for the weak conductivity of this system. The atomic orbitals involved in these two crystal orbitals are mainly $In\ 5p$ orbitals. The unit cell contains two asymmetric units and an even number of electrons. Each independent unit would have a single occupied HOMO. Symmetric and antisymmetric combinations of the two HOMO (one per unit) give rise to the two Fermi level crystal orbitals. The projected density of states does not indicate any noticeable contribution of the potassium.

The population analysis of the two crystalline phases and of the In_{11}^{7-} cluster is reported in Table 3. The excess of positive charge on alkali cations, although it should be due to numerical round-off errors occurring during the integration of the density matrix over the k points, shows that the basis functions centered

TABLE 3: Mulliken Populations^a

	K_8In_{11}	Rb_8In_{11}	In_{11}^{7-}
Atomic Net Charges			
In(1)	-0.681	-0.742	-0.124
In(2)	-0.846	-0.776	-0.527
In(3)	-0.822	-0.818	-0.929
M(36f)	1.095	1.095	
M(12c)	1.052	1.057	
Bond Population			
In(1)-In(2)	0.145	0.149	0.004
In(1)-In(3)	0.252	0.251	0.128
In(2)-In(3)	0.234	0.211	0.322
In(3)-In(3)	0.279	0.287	0.0

^a M stands for the cation.

TABLE 4: Potassium Integrated Density

radius (bohrs)	K (36f)	K (12c)	total
2.0	0.0123 ± 0.0006	0.0091 ± 0.0003	0.092 ± 0.004
2.5	0.048 ± 0.005	0.036 ± 0.005	0.36 ± 0.04
2.75	0.089 ± 0.006	0.067 ± 0.005	0.67 ± 0.05
3.0	0.136 ± 0.007	0.097 ± 0.004	1.01 ± 0.05
3.18	0.185 ± 0.008	0.137 ± 0.006	1.38 ± 0.06
3.5	0.315 ± 0.007	0.243 ± 0.005	2.38 ± 0.05
4.27	1.01 ± 0.04	0.79 ± 0.03	7.6 ± 0.3

on these atoms hardly contribute to the occupied crystalline orbitals, in agreement with the projected density of states. The differences between the net charges calculated for the naked and embedded clusters indicate that an important polarization of the charge density is induced by the electrostatic field of the cations. Without this field, the maximum net charges are found for the prismatic $In(3)$ atoms whereas those lying in the equatorial plane remain almost neutral. In the presence of the crystal field, the charge distribution is more homogeneous. The differences between the potassium and rubidium analogs are due to inequivalent cationic networks. The bond populations between indium are quite large in the solid state phases, especially for bonds involving $In(3)$ atoms. The population analysis results show that the crystal field cannot be treated as a perturbation. Therefore, the relevance of naked cluster calculations for the study of such solid state compounds is questionable.

As previously mentioned, the topological analysis of the electron density is not possible for pseudopotential calculations because atomic basins cannot be defined. However, it is always possible to construct spheres which approximate the atomic basins. The radii of these spheres are then tunable parameters which can be related to ionic, atomic, or promolecule radii.²⁵ The integrated density over such spheres evaluated by Monte Carlo integration is reported in Table 4 for the K_8In_{11} species. A sphere radius of 4.27 bohrs corresponds to the crystal radius of bulk metallic potassium, whereas K^+ ionic and promolecule radii lie in the range 2.5–2.87 bohrs.^{26,25} In principle, this sphere corresponds to the core region and is forbidden for valence electrons. The rather large integrated electron density found at 2.75 bohrs is an artifact due to large core pseudopotentials. In the actual case, the shortest K–In distance is 7.12 bohrs, and one can conjecture that the potassium basin should extend at a distance larger than 2.87 bohrs. The values of the integrated density reported in Table 4 provide a weak support to the bonding picture in which one electron is delocalized over the potassium layers. However, it is not possible to decide between that interpretation and the fully ionic one supported by the Mulliken population analysis and the projected density of states.

The localization attractors of the different species investigated have been located through a gradient search technique.²⁷ For

the two isolated clusters, there are five attractors lying on the lines joining the center of the deltahedron to the apical and equatorial indiums. Six other attractors are found, close to the In(3) atoms. Figure 1 displays the pattern of the attractors in the typical case of K_8In_{11} . For crystalline systems these attractors are outside the deltahedron whereas for the naked cluster they are inside. The distance between attractors and nearest indium centers are of the order of 1 Å. The attractors near In(3) atoms are connected by pathways similar to those encountered for metals.¹⁰ There are also such pathways between In(3) and In(2) attractors. There are neither bonding attractors nor valence attractors within the potassium layers. Moreover, the shorter distances between potassium center and indium attractors are respectively 3.24, 3.32, and 2.2 Å for In(1), In(2), and In(3). The attractors near the In(1) centers are close to the middle of the pyramids formed by one potassium and four In(3) atoms and indicates therefore a possible five-center bond involving these atoms.

The configuration of the valence attractors, though it is consistent with the weak conductivity measured for these systems, is very puzzling. It does not correspond to any well-known representation of the chemical bond. This situation corresponds to a shell of valence electrons experiencing a central potential. In the case of a spherical potential, the attractors would be degenerate on a sphere. For a one-parameter radial potential of the form

$$V(r) = -2D\left(\frac{1}{r} - \frac{1}{2r^2}\right)$$

it is possible to have a shell containing 25 electron pairs with $l = 0, 1, 2, 3$, and 4 provided $D > 2.6$ bohrs, a value which is less than the potential experienced by an electron on the surface of the deltahedron. The resolution into 11 point attractors follows from the local symmetry in the actual systems. Such a description is very close to the picture provided by the shell structure model of clusters.^{28,29} In this model, the surface electrons are subjected to an effective spherical potential which accounts for the field of all nuclei (and core electrons). The electronic structure is calculated either by DFT techniques within a jellium approximation of the density³⁰ or by a standard LCAO expansion within the tensor surface harmonic theory.³¹ This model yields maximal occupancies which depend on the geometry of the skeletal cluster. It is worth noting that our calculations and the analysis of the ELF function support the shell model and explain the quantitative success of calculations on indium clusters performed within the jellium approximation.^{32,33}

Conclusion

The results presented in this work constitute a first attempt to rationalize the question of the bonding in indium clusters by means of *ab initio* quantum chemical calculations. In agreement with experiment, the present zintl-phase structures are found to be weak conductors. At the present state of the art, the use of large core pseudopotentials hampers the electron density integration because atomic basins cannot be defined, and it is therefore not possible to decide whether or not one or more electron is delocalized over the potassium cations. The picture of the bonding is quite different from that provided by usual molecular orbital analysis but gives support to the shell model of clusters.

Acknowledgment. Financial support from Ministerio de Educación y Ciencia of Spain (DG-ICYT, Research Project PB93-0662) is gratefully acknowledged. B.S. is most indebted to Conselleria de Educació i Ciència de la Generalitat Valenciana for research funds to support his stay at Universitat Jaume I. We thank Prof. Corbett for his constant interest, Prof. von Schnerig for his suggestions, Dr. F. Colonna for providing computational assistance, and the Centre de Procesament de Dades from Universitat Jaume I for providing us with multiple computing facilities.

References and Notes

- (1) Corbett, J. D.; Sevov, S. C. *Z. Phys. D: At., Mol. Clusters* **1993**, 26, 64.
- (2) van der Lugt, W. *Phys. Scr.* **1991**, 39, 372.
- (3) de Heer, W. A.; Knight, W. O.; Cham, M. Y.; Cohen, M. L. In *Solid State Physics*; Ehrenreich, H., Turnbull, E., Eds.; Academic Press: New York, 1987; Vol. 40.
- (4) Mingos, D. P. M.; Wales, D. J. *Introduction to Cluster Chemistry*; Prentice-Hall: Englewood Cliffs, NJ, 1990.
- (5) Burdett, J. K.; Canadell, E. J. *Am. Chem. Soc.* **1990**, 112, 7207.
- (6) Sevov, S. C.; Corbett, J. D. *Science* **1993**, 262, 880.
- (7) Sevov, S. C.; Corbett, J. D. *Inorg. Chem.* **1991**, 30, 4876.
- (8) Blase, W.; Cordier, G.; Müller, V.; Häussermann, U.; Nesper, R. *Z. Naturforsch.* **1992**, 48B, 754.
- (9) Zintl, E.; Neumeyst, S. *Z. Phys. Chem. (Munich)* **1933**, 272.
- (10) Silvi, B.; Savin, A. *Nature* **1994**, 371, 683.
- (11) Frisch, M. J.; Trucks, G. W.; Schlegel, H. B.; Gill, P. M. W.; Johnson, B. G.; Wong, M. W.; Foresman, J. B.; Robb, M. A.; Head-Gordon, M.; Repogle, E. S.; Gomperts, R.; Andres, J. L.; Raghavachari, K.; Binkley, J. S.; Gonzalez, C.; Martin, R. L.; Fox, D. J.; Defrees, D. J.; Baker, J.; Stewart, J. J. P.; Pople, J. A. *Gaussian 92/DFT, Revision F.4*; Gaussian, Inc.: Pittsburgh, PA, 1993.
- (12) Durand, P.; Barthelat, J. C. *Theor. Chim. Acta (Berlin)* **1975**, 38, 283.
- (13) Bouteiller, Y.; Mijoule, C.; Nizam, M.; Barthelat, J. C.; Daudey, J. P.; Pelissier, M.; Silvi, B. *Mol. Phys.* **1988**, 65, 295.
- (14) Becke, A. D. *J. Chem. Phys.* **1988**, 98, 5648.
- (15) Lee, C.; Yang, Y.; Parr, R. G. *Phys. Rev.* **1988**, B37, 785. Miehlich, B.; Savin, A.; Stoll, H.; Preuss, H. *Chem. Phys. Lett.* **1989**, 157, 200.
- (16) Dovesi, R.; Saunders, V. R.; Roetti, C. *CRYSTAL 92, An ab initio HF LCAO program for periodic systems*. Theoretical Chemistry Group, University of Turin, Italy; SERC Daresbury Laboratory, UK, 1992.
- (17) Jeung, G. H. *Phys. Rev.* **1987**, A35, 26.
- (18) Pisani, C.; Dovesi, R.; Roetti, C. *Hartree-Fock Ab-initio Treatment of Crystalline Systems (Lecture Notes in Chemistry)*; Springer-Verlag: Berlin, 1988.
- (19) Blase, W.; Cordier, G.; Somer, M. Z. *Kristallogr.* **1991**, 194, 150.
- (20) Cordier, G.; Müller, V. Z. *Kristallogr.* **1991**, 194, 154.
- (21) This is due to the fact that for a scalar generating function (also called potential function) the limit points of its gradient field are nodal hyperbolic points (see Abraham and Shaw, *The Geometry of Behavior*, Visual Mathematical Library).
- (22) Bader, R. F. W. *Atoms in Molecules. A Quantum Theory*; Clarendon: Oxford, 1990.
- (23) Becke, A. D.; Edgecombe, K. E. *J. Chem. Phys.* **1990**, 92, 5397.
- (24) Savin, A.; Jepsen, O.; Flad, J.; Andersen, O. K.; Preuss, H.; von Schnering, H. G. *Angew. Chem.* **1992**, 31, 187.
- (25) Cooper, D. L. *Nature* **1994**, 371, 651.
- (26) Feth, S.; Gibbs, G. V.; Boisen, M. B., Jr.; Myers, R. H. *J. Phys. Chem.* **1993**, 97, 11445.
- (27) Shannon, R. D. *Acta Crystallogr.* **1976**, A32, 751.
- (28) Colonna, F. Private communication.
- (29) Wales, D. J.; Mingos, D. M. P.; Slee, T.; Zhenyang, L. *Acc. Chem. Res.* **1990**, 23, 17.
- (30) Martin, T. P.; Bergmann, T.; Göhlich, H.; Lange, T. *J. Phys. Chem.* **1991**, 95, 6421.
- (31) Chou, M. Y.; Cohen, M. L. *Phys. Lett.* **1986**, A113, 420.
- (32) Stone, A. J. *Mol. Phys.* **1980**, 41, 1339.
- (33) Onwuagba, B. N. *Phys. Status Solidi: B* **1993**, 180, 391.
- (34) Baguenard, B.; Pellarin, M.; Bordas, C.; Lermé, J.; Vialle, J. L.; Broyer, M. *Chem. Phys. Lett.* **1993**, 205, 13.